Experimental observation of light refraction going from negative to positive in the visible region at the pure air/Au interface

Yun-Hua Wu, Wen Gu, Yue-Rui Chen, Xiao-Fan Li, Xiao-Song Zhu, Peng Zhou, Jing Li, Yu-Xiang Zheng, and Liang-Yao Chen*

State Key Laboratory of Advanced Photonic Materials and Devices, Department of Optical Science and Engineering, Fudan University, Shanghai 200433, China

(Received 11 May 2007; published 31 January 2008)

We report wavelength-dependent refraction going from negative to positive in the visible region for the pure air/Au interface by fabricating a series of prismlike Au film samples. Results qualitatively agree with dispersion of the group refractive index n_g, in which the spectral properties of the phase refractive index n_p, play a significant role to make both the magnitude and sign of n_g change in the energy region where interband transitions occur. The net refraction observed for the simplest air and metal interface will stimulate further exploration of the physical origin of slow or fast light characterized by the law of refraction in nature.

DOI: 10.1103/PhysRevB.77.035134 PACS number(s): 78.20.Ci, 78.66.Bz

I. INTRODUCTION

Light propagated in vacuum with the velocity c will change its velocity to $v=c/n$ after interacting with a medium, as characterized by the optical refractive index n. There are three types of light, referred to as slow light ($n>1$), fast light ($n<1$), and light with a negative velocity ($n<0$).[1–3] With respect to the transmission of energy, phase, and information of the light, respectively, three types of light velocity are suggested: the group velocity $v_g=c/n_g$, phase velocity $v_p=c/n_p$, and information velocity $v_i=c/n_i$.[1] To preserve causality, the information refractive index $n_i=1$ in all situations.[1,4] The phase refractive index n_p, equals the normal refractive index n, and can be smaller than 1 for metals.[5] The magnitude and sign of the group refractive index n_g ($n_g=n+Edn/dE$),[1]however, will depend on the dispersive feature of dn/dE, which will vary with the photon energy E. Negative group refraction can occur for the condition in which $dn/dE<1$ and $|Edn/dE|>n$. Negative light refraction was observed recently in artificially composed materials[6] and generated serious discussions and controversies over its physical origin[7–14] due to the lack of reliable dispersive knowledge of the refractive index measured for materials in the microwave region. By overcoming the extreme difficulty due to very short light penetration depth in the metal, we carried out the experiment to measure the light refraction and find that the light refraction changes from negative to positive, by crossing zero, at a simple and pure air/Au interface in the visible region. Our observation agrees with the prediction of the group velocity based on the dispersive feature of the phase refractive index, and will advance understanding of, and resolve the controversies over, the complicated light refraction phenomena which occur at the dielectric or metal interface.

II. EXPERIMENT

The pseudorefraction caused by multiple absorptions, refractions, and deflections in the artificial structure actually do not present the law of refraction. Therefore, a significant approach has been suggested to study the net refraction effect[13] of the single dielectric and metal interface by excluding side effects[14] possibly induced in the artificially composed structure. In this work, a series of prismlike Au film samples with purity of 99.99% were rf (radio frequency) sputtered on the double-side-polished plane glass substrate in the Leybold-600SP chamber at room temperature. The samples were prepared to have variable wedge-shaped angles of θ_m. The Au sample is relatively stable in room atmosphere and has a complex refractive index $\tilde{n}_m$ ($\tilde{n}_m=n+ik$, where n and k are the refractive index and extinction coefficient, respectively) in the visible region. The base pressure is about 7×10^{-6} mbar and the film growth rate is about 0.128 nm/s, as cross checked and calibrated (to within an error of about $\pm2\%$) by the Kosaka Surfcorder ET300 and weight measurement. In terms of the microstepping motor working in the vacuum chamber, the angle of θ_m was controlled by the computer to *in situ* adjust the linear movement of the mask over the sample. The spectra of the real and imaginary parts of the complex dielectric constant $\varepsilon(\varepsilon=\varepsilon_1+i\varepsilon_2)$ of the thick film sample were ellipsometrically measured in the 1.5–4.5 eV photon energy range.[15] The higher ε_2 values in the interband transition region ($\varepsilon_2=6.667$ at 3.8 eV) indicate that the rf-sputtered sample has a higher film density.[16]

As shown in Fig. 1, two solid lasers with the wavelength $\lambda=473.0$ and 532.0 nm, and one He-Ne laser with wavelength $\lambda=632.8$ nm, were used with the beam deviation down to less than about 0.3 mrad by using a 20× beam expander. Two apertures with diameters of 2 mm were used to let the laser beam pass through. The measured complex refractive indices $\tilde{n}_m$ for the film sample are $\tilde{n}_m=1.313+i1.73$, $0.429+i2.028$, and $0.193+i3.524$ at the wavelengths $\lambda=473.0$, 532.0, and 632.8 nm, respectively. The laser beam was incident onto the glass side of the sample along the z direction normal to the Au and glass interface and was out at the oblique air and Au interface. The beam transmitted through the film was multiply reflected between two plane mirrors to extend the optical path (by tenfold) and make the image show on the screen located at a distance ($L=20.55$ m) away from the sample. The size and shape of the beam image were measured by a CCD (charge-coupled device) camera with a 12-bit A/D converter resolution.

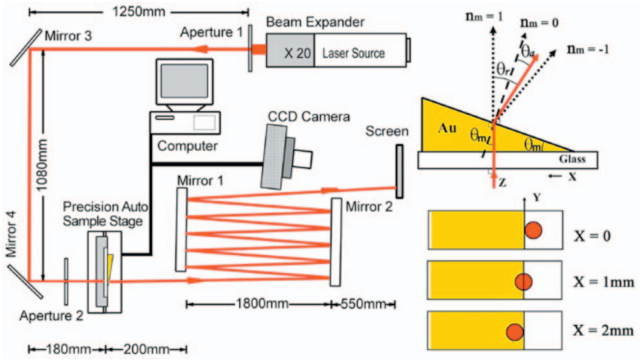

FIG. 1. (Color) The experimental setup to measure the refraction of light which was transmitted through the wedged-shaped Au and *a*-Si thin films at different *x* positions. The CCD camera was used to record the transmitted beam spot which was imaged on the screen with the light path extended by ten multiple reflections of the light between two plane mirrors, 1 and 2, that have a length of about 200 mm.

A precision displacement stage was controlled by the computer to move the sample along the *x* direction. The positions of $x=0$ and $x=2.2$ mm imply the situations in which the laser beam just touches the thinner edge of the film and fully transmits through the film, respectively, to avoid side effects such as edge deflection, interference, scattering, and so on. The beam image size and shape were quantitatively recorded by the camera as the sample was scanned by the laser beam crossing the thin edge of the film. The two-dimensional intensity distribution of the laser beam measured by the camera was integrated in the *y* direction to extract the intensity distribution along the *x* direction. Afterwards, the peak position was determined by measuring the center position of the full width at half maximum (FWHM) of the light intensity distribution along the *x* direction. As the beam transmits through the wedge-shaped film, either the small left (+) or right (−) refraction angle of $\pm\theta_r$ with respect to the *z* axis was measured by the CCD camera with a resolution of 27.4 pixels/mm, as calibrated by scaling the real beam image size shown on the screen.

III. RESULTS AND DISCUSSIONS

As seen in Fig. 2(a), the transmitted light intensity at $\lambda=473.0$, 532, and 632.8 nm decreases significantly as the beam fully enters into the Au film ($\theta_{m,\mathrm{Au}}=77.5$ μrad used here illustrates a typical case) at $x=2.2$ mm. The peak position P_{Au} of the Au sample is shifted to the left and right side, respectively, as compared to the original intensity distribution measured at the position $x=0$. As a comparison, the measurement also was made on a wedge-shaped amorphous Si (*a*-Si) film sample ($\theta_{m,a\text{-Si}}=27.3$ μrad) which was sputtered on the glass substrate. The result shows the pure left shift of the peak position $\mathrm{P_{Si}}(x=2.2$ mm) with decreasing intensity of the light. The peak position shift of the beam intensity was measured by $\Delta P=[P(x=0)-P_{\mathrm{shift}}(x=2.2\ \mathrm{mm})]_{L=20.55\ \mathrm{m}}$ at the beam spot location $L=20.55$ m and at $\lambda=473.0$, 532.0, and 632.8 nm, respectively, with the same experiment procedure.

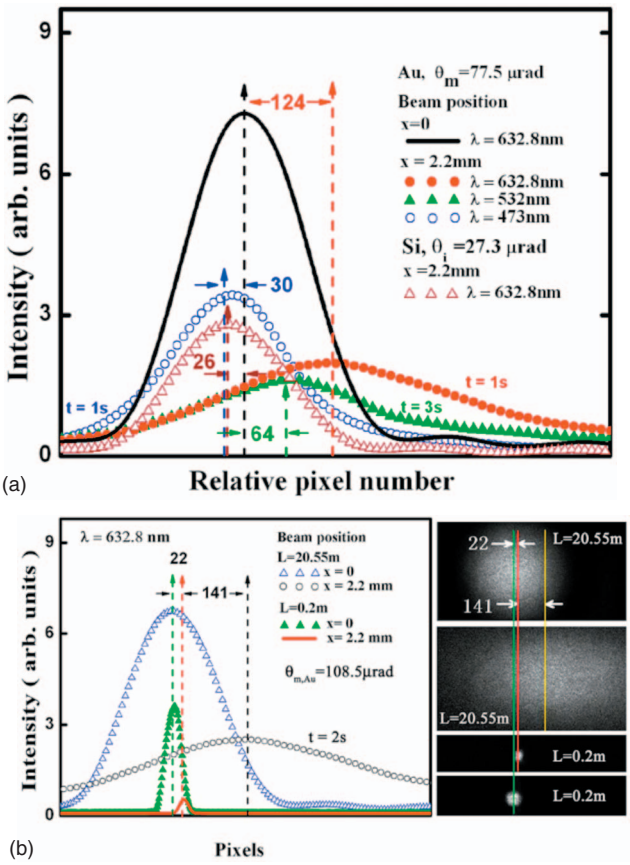

FIG. 2. (Color) The measured light intensity distributions along the *x* direction show the positive and negative light refraction as recorded with the pixel numbers by the CCD camera for the wedged *a*-Si and Au film samples, respectively. (a) The left peak shifts by 26 pixels for *a*-Si ($\theta_{m,a\text{-Si}}=27.3$ μrad, $\lambda=632.8$ nm, $t=0.1$ s) and by 30 pixels for Au ($\theta_{m,\mathrm{Au}}=77.5$ μrad, $\lambda=473.0$ nm, $t=1$ s); the right peak intensity shifts by 30 pixels ($\lambda=532.0$ nm, $t=3$ s) and 124 pixels ($\lambda=632.8$ nm, $t=1$ s with the intensity amplified by ten times) for the same Au sample. (b) The parallel shift (22 pixels) and the net refraction (141 pixels) were measured by carefully analyzing the beam image for the Au sample ($\theta_{m,\mathrm{Au}}=108.5$ μrad, $\lambda=632.8$ nm) at $L=0.2$ m ($t=0.1$ s with an intensity attenuator) and $L=20.55$ m ($t=2$ s with the intensity amplified by 20 times), respectively.

The attenuation of the light intensity in the wedge-shaped Au film will be not uniform along the *x* direction. This will induce a peak shift $\Delta\xi$ in the light emerging from the air and Au interface that confounds the near-field data analysis for the case in which the detector is too close to the thick film sample (about 2-μm-thick in the middle[17]). This effect will not refract the light, but will cause a parallel displacement of the peak intensity within the maximum shift, $\leq 1/2$ beam size (≤ 1 mm in this work), depending on the thickness and wedged angle of the sample. The parallel shift of $\Delta\xi=[P(x=0)-P_{\mathrm{shift}}(x=2.2\ \mathrm{mm})]_{L=0.2\ \mathrm{m}}$ was measured and analyzed for each sample by using the CCD camera to measure the distribution of the transmitted beam intensity imaged on the screen at the location $L=0.2$ m away from the sample at $\lambda=473.0$, 532.0, and 632.8 nm, respectively. The net shift of the beam position then can be obtained as $\Delta P_{\mathrm{net}}=\Delta P-\Delta\xi$.

The measured parallel shift of $\Delta\xi$(22 pixels$\cong$0.8 mm) at λ =632.8 nm and the net shift ΔP_{net}(141 pixels$\cong$5.15 mm) of the beam intensity for the sample ($\theta_{m,\text{Au}}$=108.5 μrad) are typically shown in Fig. 2(b).

Beam expansion through the wedged film was observed. This is not due to microscattering effects, in contrast to the situations in which the light beam goes through the glass substrate and plane Au thin film, respectively, where no beam size expansion effect happened. The expansion effect can be attributed to a nonuniform distribution of the electrical field at the wedged air and metal interface with narrowed beam size. The absorption of the beam at λ=632.8 nm is also higher than that at λ=532.0 and 473.0 nm to make the beam size at x=2.2 mm (λ=632.8 nm) narrower than that at other wavelengths. It can be seen that this effect results in the beam profile being broader at λ=632.8 nm than that at the other two wavelengths.

Afterwards, the angle $\theta_r(x) \approx (\Delta P_{\text{net}}/L)_{L=20.55\ \text{m}}$ was obtained to further extract the refraction angle $\theta_a(x)=\theta_r(x)-\theta_m$. Results are shown in Fig. 3(a) for the samples that were repeatedly measured, back and forth ten times, at the x=0 and 2.2 mm positions (over a short period of time to avoid errors arising from possible air disturbance and vibration in the room atmosphere).

For the small angles of θ_a and θ_m, Snell's law will be approximated as $\theta_a=n_m\theta_m$. As seen in Fig. 3(a), θ_a is positive at 473.0 nm and negative at 532.0 and 632.8 nm wavelengths. Linear regression, shown as the dashed lines, reveal an average $n_{m\text{-Au}}=1.488\pm0.11$, -0.34 ± 0.10, and -1.56 ± 0.18 at λ=473.0, 532.0, and 632.8 nm, respectively.

The complex refractive index $\tilde{n}_m$ of the metal-based material is physically correlated to the complex dielectric function $\varepsilon=\tilde{n}_m^2$ ($\varepsilon_1=n^2-k^2$ and $\varepsilon_2=2nk$). The energy loss function is proportional to $\text{Im}(-1/\varepsilon)=\varepsilon_2/(\varepsilon_1^2+\varepsilon_2^2)$, which is positive. Without considering the core dielectric response in the higher energy limit, the real part of the complex dielectric function of the metal is that

$$\varepsilon_1 = 1 - \omega_p^2/\omega^2 = 1 - 2\int_0^\infty \omega'\varepsilon_2 d\omega'/\pi\omega^2, \qquad (1)$$

where ω_p is the plasma frequency.[18] In the energy range of $\omega<\omega_p$, $\varepsilon_1<0$, and $k>n$, this implies high optical absorption with very short light penetration depth δ ($\delta=\lambda/4\pi k$), as compared to the wavelength. The overall integral in the equation implies that the optical constant is strongly influenced by the electromagnetic energy loss over the entire frequency range due to the microphysical processes related to internal electron scattering, intraband and interband transitions, and so on. The real and imaginary parts of the complex wave vector will not align along the same direction in the inhomogeneous electric field of the metal.[19] According to the theory, the surfaces of constant amplitude and phase will not coincide as the light is obliquely incident from the dielectric media onto the metal,[19] but will coincide with each other along the same direction in the reversed light path as arranged in this work.

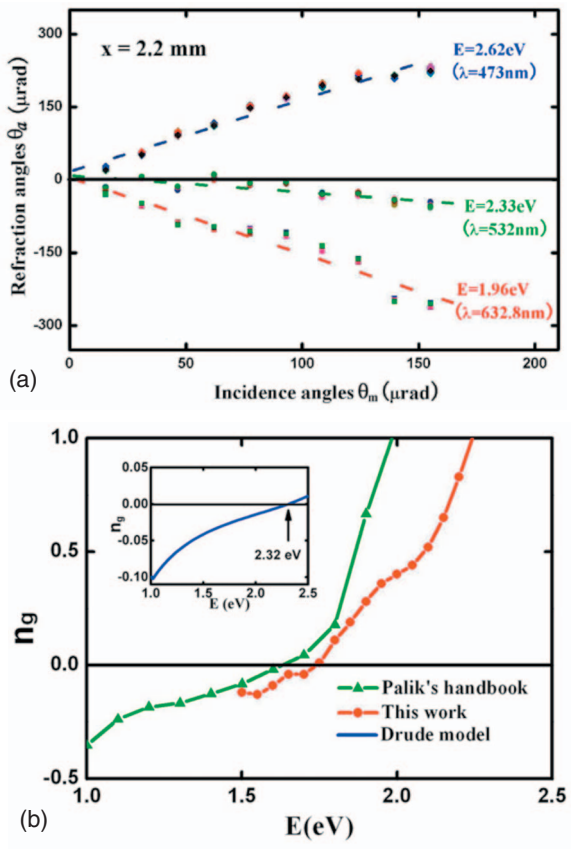

FIG. 3. (Color) (a) In terms of Snell's law, the measured net refractions for the pure air and Au interfaces show that the refractive index n_m of Au changes from negative to positive, with the dashed lines giving average values by taking linear regression of the data, i.e., $n_{m\text{-Au}}=-1.56\pm0.18$, -0.34 ± 0.10, 1.488 ± 0.11 at λ =632.8, 532.0, and 473.0 nm, respectively. (b) The group refractive index n_g is numerically calculated from the data from Palik's handbook and this work, respectively. The inset shows the numerically calculated spectrum of the group refractive index n_g, based on the Drude model.

At the dielectric and metal interface, the actual energy flow of the light will be along the real physical angle of θ_m. Therefore, the generalized Snell's law is

$$n_a \sin\theta_a = \tilde{n}_m \sin\tilde{\theta}_m \qquad (2)$$

that can be modified to $n_a \sin\theta_a = n_m \sin\theta_m$ (Refs. 19 and 20) where both n_m and θ_m are real and can be measured in the experiment. Two sets of equations were developed to deal with the situations for light entering from the dielectric medium to metal[19] and vice versa.[20] The detailed calculations for the plane film structures (air/glass/Au/air or air/Au/glass/air) show that the predicted light path θ_m or n_m, will not be reversible and continuous in all angle conditions. The nonsymmetrical light path at the Au and air interface, as expected in theory, is not in agreement with the experimental observations. Also at the very small incidence angle condition, the calculated value of n_m will be positive and $n_m \approx n$ as shown by those equations[19,20] that are not in agreement with the experimental observation in this work.

To explain the origin of negative refraction for the metal-based artificial material, in which a noble metal like Au is often used as the key element,[6,21] the assumptions of the magnetic permeability, $\mu \neq 1$ or $\mu < 0$, have to be applied,[22] though not exactly measured and confirmed by experiment.[21,23] Based on the Maxwell-Garnett (MG) model, for the artificial material composed of a metal and dielectric medium in the visible region, the effective dielectric constant ε_e ($\varepsilon_e = \varepsilon_{e1} + i\varepsilon_{e2}$), and permeability μ_e ($\mu_e = \mu_{e1} + i\mu_{e2}$), can be approximately expressed as $(\varepsilon_e - \varepsilon)/(\varepsilon_e + \varepsilon) = (\varepsilon_m - \varepsilon) f_s/(\varepsilon_m + \varepsilon)$ and $\mu_e = (1 - f_s)\mu + f_s \mu_m$, respectively, where ε and μ are the dielectric constant and magnetic permeability of the host matrix medium, respectively, ε_m and μ_m are the complex dielectric constant and magnetic permeability of the metal element embedded in the matrix, and f_s is the filling factor.[24] The effective refractive constant is $\tilde{n}_e$ ($\tilde{n}_e = n_e + ik_e$) with the relation of that $\tilde{n}_e^2 = \varepsilon_e \mu_e$. It is well known that the d band is full and only the s-band electrons in the noble metal will be mainly interacting with the electromagnetic field in the intraband transition region. Also, unlike the electron dipole moment, the magnetic dipole moment cannot be followed effectively with the electromagnetic field to vibrate in the high optical frequency. Therefore, μ_m should equal 1 for the noble metals in the visible region.[18,19] The magnetic permeability of the nonmagnetic dielectric medium forming the matrix also equals 1 in the visible region, resulting in the following: $\mu_e = \mu = 1$, $\tilde{n}_e^2 = \varepsilon_e$, $n_e^2 - k_e^2 = \varepsilon_{e1}$, and $2n_e k_e = \varepsilon_{e2}$. The value of the effective dielectric constant ε_e will depend on the geometric shape and size of the metal element and filling factor.[25] However, if the metal and dielectric medium all have positive imaginary parts of the dielectric constant in the visible region, the effective k_e and ε_{e2} will be positive, resulting in a positive effective n_e for the composed artificial material.

It has been studied and predicted recently that the negative displacement of the beam transmitted through a nonabsorptive medium[26] or a thin metal film[27] can happen due to internal reflections at the interface induced by the Goos-Hänchen effect that depends on the polarization of the incident light. At the very small incidence angle condition, however, the effect can be omitted and the refraction observed in this work is independent on the polarization of the light and changes its sign from negative to positive with the wavelength in the visible region.

For a pure metal like Au, the group velocity represents the energy flow of the light associated with the group refractive index n_g, which can be negative with an anomalous dispersion feature of n in the resonance region.[14,28,29] The larger negative n_g also was studied and observed for other dispersive media in the resonance energy region.[30,31] There are intraband and interband transitions coexisting in the visible region of Au to give the anomalous dispersion feature of the refractive index n as

$$n = \sqrt{(\sqrt{\varepsilon_1^2 + \varepsilon_2^2} + \varepsilon_1)/2} \tag{3}$$

for which $dn/dE < 0$. The Drude intraband transitions that are dominated in the low energy region will be mixed with the interband transitions to make the resonance of energy loss happen at a photon energy of about 2.5 eV.[5,16,18] In the tail of the Drude region, the real and imaginary parts of the dielectric function can be presented as

$$\varepsilon_1 = \varepsilon_\infty - E_p^2/E^2, \quad \varepsilon_2 = E_p^2 \hbar / E^3 \tau, \tag{4}$$

where ε_∞, E_p, and τ are the dielectric constant at the high energy limit, plasma energy, and relaxation time, respectively. By taking the film data of the Au sample, $\varepsilon_\infty = 8.13$, $E_p = 9.33$ eV, and $\tau = 2.7 \times 10^{-14}$ s,[16] the spectrum of the group refractive index n_g was numerically calculated in the 1.0–2.5 eV region with the result shown in the inset of Fig. 3(b). The numerical calculations also were made based on the data of the refractive index given in Ref. 5 as well as that measured in this work, with the results shown in Fig. 3(b). It can be seen that n_g does change from negative to positive with increasing photon energy in the visible region. The zero of n_g occurs around 1.7 eV for the calculation based on the data given in Ref. 5 and that measured in this work, and at about 2.32 eV for the calculation based on the Drude model. The disagreement may arise from the fact that the refractive index given in Ref. 5 and this work are measured in the wavelength region, where the long tail of the interband transitions will have some mixing with the intraband transitions to affect the data, but the simulation (inset) considers the intraband transitions based on the pure Drude model only.

The numerically calculated spectra of the group refractive index based on the data of the refractive index and the Drude model are qualitatively in agreement with the measured ones, since the refraction index n_m observed in this work is associated with the energy flow of light which can be related to the dispersive feature of n_g. It goes from more negative at $\lambda = 632.8$ nm ($E = 1.96$ eV) to less negative at $\lambda = 532.0$ nm ($E = 2.33$ eV), and passing through zero to be positive at $\lambda = 473.0$ nm ($E = 2.62$ eV). Results indicate that the zero $n_g$will occur at the region close to the resonance energy, between 2.33 eV and 2.62 eV, where the onset ($E \approx 2.5$ eV) of interband transitions occurs and the anomalous dispersion of the phase refractive index n changes with the photon energy. In the high energy region ($E > 2.5$ eV), $\varepsilon_2 \gg |\varepsilon_1|$, $n \approx k \approx (\varepsilon_2/2)^{1/2}$, $dn/dE > 0$, and $n_g > 0$ due to increasing of ε_2 with the photon energy in the region close to and above the onset of the interband transitions occurring in Au.[5,16] The property of net light refraction going from negative to positive observed at the pure Au and air interface in the visible region, therefore, will explore and aid in understanding the origin of the effect occurring for Au-embedded artificial materials in other optical frequency ranges.

IV. CONCLUSION

We experimentally show that light refraction can go from negative to positive at pure air and Au interfaces in the visible region in this work. Results qualitatively agree with dispersion of the group refractive index n_g based on the refractive index and a Drude model, in which the dispersive properties of the phase refractive index n play the significant role to make n_g change its magnitude and sign in the energy

region, due to the microinteractions between the photons and electrons with respect to the intraband and interband transitions in the material. The net refraction observed for the simplest air and metal interface will stimulate further exploration of the physical origin of slow or fast light characterized by the law of refraction in nature.

ACKNOWLEDGMENTS

This work was supported by the NSF projects of China with the Contracts No. 60277031 and No. 60327002. The authors thank Lei Xu and Zhong-Hong Dai for the support of laser facilities and measurement in the experiment.

*lychen@fudan.ac.cn

[1] M. D. Stenner, D. J. Gauthier, and M. A. Meifeld, Nature (London) **425**, 695 (2003).
[2] M. D. Stenner and D. J. Gauthier, Phys. Rev. A **67**, 063801 (2003).
[3] K. Kim, H. S. Moon, C. Lee, S. K. Kim, and J. B. Kim, Phys. Rev. A **68**, 013810 (2003).
[4] R. Y. Chiao and A. M. Steinberg, *Progress in Optics*, edited by E. Wolf (Elsevier, Amsterdam, 1997), Vol. 37, Chap. 6, p. 345.
[5] D. W. Lynch and W. R. Hunter, *Handbook of Optical Constants of Solids*, edited by E. D. Palik (Academic Press, London, 1985), p. 275.
[6] R. A. Shelby, D. R. Smith, and S. Schultz, Science **292**, 77 (2001).
[7] E. Cubukcu, K. Aydin, E. Ozbay, S. Foteinopoulou, and C. M. Soukoulis, Nature (London) **423**, 604 (2003).
[8] P. V. Parimi, W. T. Lu, P. Vodo, J. Sokoloff, J. S. Derov, and S. Sridhar, Phys. Rev. Lett. **92**, 127401 (2004).
[9] Z. Lu, S. Shi, C. A. Schuetz, and D. W. Prather, Opt. Express **13**, 2007 (2005).
[10] S. Zhang, W. Fan, N. Panoiu, K. Malloy, R. Osgood, and S. Brueck, Phys. Rev. Lett. **95**, 137404 (2005).
[11] J. B. Pendry, Nature (London) **423**, 22 (2003).
[12] P. M. Valanju, R. M. Walser, and A. P. Valanju, Phys. Rev. Lett. **88**, 187401 (2002).
[13] N. Garcia and M. Nieto-Vesperinas, Opt. Lett. **27**, 885 (2002).
[14] H. Shin and S. Fan, Phys. Rev. Lett. **96**, 073907 (2006).
[15] L. Y. Chen, X. W. Feng, Y. Su, H. Z. Ma, and Y. H. Qian, Appl. Opt. **33**, 1299 (1994).
[16] D. E. Aspnes, E. Kinsbron, and D. D. Bacon, Phys. Rev. B **21**, 3290 (1980).
[17] M. Sanz, A. Papageorgopoulos, W. F. Egelhoff, M. Nieto-Vesperinas, and N. Garcia, Phys. Rev. E **67**, 067601 (2003).
[18] F. Wooten, *Optical Properties of Solids* (Academic Press, New York/London, 1972), Chap. 2-3.
[19] M. Born and E. Wolf, *Principles of Optics*, 6th ed. (Pergamon Press, Oxford, 1993), Chap. 13.
[20] J. L. Garcia-Pomar and M. Nieto-Vesperinas, Opt. Express **12**, 2081 (2004).
[21] A. N. Grigorenko, A. K. Geim, H. F. Gleeson, Y. Zhang, A. A. Firsov, I. Y. Khrushchev, and J. Petrovic, Nature (London) **438**, 335 (2005).
[22] V. M. Shalaev, Nat. Photonics **1**, 41 (2007).
[23] A. V. Kildishev, V. P. Drachev, U. K. Chettiar, D. Werner, D. H. Kwon, and V. M. Shalaev, arXiv:physics/0609234 (unpublished).
[24] X. H. Hu, C. T. Chan, J. Zi, M. Li, and K. M. Ho, Phys. Rev. Lett. **96**, 223901 (2006).
[25] D. E. Aspnes, Am. J. Phys. **50**, 704 (1982).
[26] H. M. Lai, C. W. Kwok, Y. W. Loo, and B. Y. Xu, Phys. Rev. E **62**, 7330 (2000).
[27] G. Dolling, M. W. Klein, M. Wegener, A. Schädle, B. Kettner, S. Burger, and S. Linden, Opt. Express **15**, 14219 (2007).
[28] M. V. Klein and T. E. Furtak, *Optics*, 2nd ed. (Wiley, New York, 1986), p. 629.
[29] G. Dolling, C. Enkrich, M. Wegener, C. M. Soukoulis, and S. Linden, Science **312**, 892 (2006).
[30] J. Peatross, S. A. Glasgow, and M. Ware, Phys. Rev. Lett. **84**, 2370 (2000).
[31] A. M. Akulshin, S. Barreiro, and A. Lezama, Phys. Rev. Lett. **83**, 4277 (1999).